# NIH RELAIS Document Delivery

NIH-10286762

JEFFDUYN

NIH -- W1 MA34IF

JOZEF DUYN
10 Center Dirve
Bldg. 10/Rm.1L07
Bethesda, MD 20892-1150

ATTN:
PHONE: 301-594-7305
FAX: -
E-MAIL:

SUBMITTED: 2002-08-29 17:22:18
PRINTED: 2002-09-03 07:36:59
REQUEST NO.:NIH-10286762
SENT VIA: LOAN DOC
7967424

---

NIH Fiche to Paper Journal

---

TITLE: MAGNETIC RESONANCE IN MEDICINE : OFFICIAL JOURNAL OF THE SOCIETY OF MAGNETIC RESONANCE IN MEDICINE / SOCIETY OF MAGNETIC RESONANCE IN MEDICINE
PUBLISHER/PLACE: Wiley-Liss, Inc., a division of John Wil New York, NY :
VOLUME/ISSUE/PAGES:1994 Sep;32(3):429-32 429-32
DATE: 1994
AUTHOR OF ARTICLE: Duyn JH; van Gelderen P; Liu G; Moonen CT
TITLE OF ARTICLE: Fast volume scanning with frequency-shifted BURST
ISSN: 0740-3194
OTHER NOS/LETTERS: Library reports holding volume or year
8505245
7984078
SOURCE: PubMed
CALL NUMBER: W1 MA34IF
REQUESTER INFO: JEFFDUYN
DELIVERY: E-mail: jhd@helix.nih.gov
REPLY: Mail:

# Fast Volume Scanning with Frequency-Shifted BURST MRI

Jeff H. Duyn, Peter van Gelderen, Guoying Liu, Chrit T.W. Moonen

**We introduce a modified BURST imaging technique with reduced saturation effects and improved signal-to-noise ratio. The method applies a frequency shift to the RF excitation pulse on successive repetitions. It allows collection of 3D datasets of human brain within a few seconds, on a standard clinical scanner at 1.5 Tesla.**

**Key words: MRI, BURST, fast MRI, brain.**

## INTRODUCTION

Over the past few years, interest has grown in fast imaging techniques. In particular, the recent exploitation of contrast mechanisms based on physiology dependent microscopic susceptibility ($T_2$*) effects (1, 2) has resulted in an explosive growth of the field of MR neuro-imaging, and has led to increasing demands on $T_2$* sensitized fast MRI. Among the most popular techniques are echo-planar imaging (EPI) (3), FLASH (4) and echo-shifted FLASH (ES-FLASH) (5), each with its own advantages and disadvantages.

BURST imaging is a class of ultra fast imaging techniques proposed by Hennig (6, 7). Versions with an improved signal-to-noise ratio (SNR) have been proposed by Le Roux *et al.* (8), Lowe and Wysong (9), and Zha *et al.* (10). Conventional BURST excites a set of equally spaced, narrow strips within an object, and creates an image from a single slice, perpendicular to the direction of the strips. In order to average, to scan multiple slices, or for 3D imaging, repeated excitation of the same strips is required. For ultra fast scanning, repetition times are short compared with the longitudinal relaxation time, leading to saturation effects and thus efficiency loss. In addition, when scanning in a 2D mode, the commonly used slice selective RF refocusing pulse also leads to additional saturation. In the following, we propose a method, called frequency-shifted BURST (or FS-BURST), which overcomes these problems by shifting the location of the excited strips on successive repetitions.

## METHODS

All experiments were performed on a standard 1.5 T GE/SIGNA clinical scanner (GE Medical Systems, Milwaukee), equipped with 10 mT/m, actively shielded whole body gradients. A standard quadrature head RF coil was used. The maximum RF output power was 2 kW, and the RF dwell time was 2 μs. The receiver had a bandwidth of 125 kHz (complex points). The human subject protocol was approved by the intramural review board of the National Institute of Mental Health at NIH.

The pulse sequence used for 3D FS-BURST is given in Fig. 1. Excitation of magnetization was performed with a BURST type RF pulse (initially introduced in high resolution spectroscopy (11), and often referred to as "DANTE pulse") in combination with a slice selection gradient. Since a DANTE pulse by itself leads to excitation of spins within narrow frequency bands, its combination with a slice selection gradient will lead to selection of narrow strips in the object under study. This principle is illustrated in Figs. 2 and 3a. The BURST pulse consisted of a train of 48 evenly spaced RF pulses. To improve the RF frequency profile and the resulting strip profile, a Hamming filter was applied over 50% of the pulse train. The individual RF pulses were 128 μs long, and were apodized with a combination of a double sidelobed sinc and a Gaussian function to improve the profile of the selected slab. The pulse spacing was 384 μs, total BURST pulse length 18.2 ms. The selection gradient was applied simultaneously in anterioposterior and superior-inferior directions, using maximum gradient strength in both directions. This resulted in selection of a 120-mm thick slab with 45° angulation. The total nutation angle of the BURST pulse was between 70° and 90° for the center of each strip. An echo train of 48 echoes was generated for each of the two reversals of the selection gradient. Forty-eight data points were acquired per echo, and the echoes were phase encoded in the left-right direction by application of a continuous gradient (PE-1 in Fig. 1). Also this gradient was reversed on subsequent echo trains. Effective echo times of first and second echo train were 19.7 and 42.5 ms, respectively. A third gradient direction (combination of posterior-anterior and superior-inferior, PE-2 in Fig. 1) was used to phase encode the subsequent repetitions. Also, on subsequent repetitions, incremental offsets were added to the RF-frequency to effectively shift the location of the excited strips (Fig. 3b). Two different shifting protocols were used: the first one used a shift of a single strip width, the second one used a shift of seven strip widths (modulo 48) on successive scans. The repetition time ($TR$) was 65 ms. A 48 × 48 × 48 data matrix was collected using a 21 cm × 21 cm × 22 cm field of view (FOV). The 22-cm FOV was used in the slice select direction and was limited by the maximum effective gradient strength of 14 mT/m. The total measurement time was 3.1 s. For repeated scans, a wait period of 15 s was observed to prevent

**MRM 32:429–432 (1994)**

From the Laboratory of Diagnostic Radiology Research, OIR, NIH, Bethesda, Maryland (J.H.D.); and NIH In Vivo NMR Research Center, BEIP, NCRR, National Institutes of Health (J.H.D., P.v.G., G.L., C.T.W.M.).

Address correspondence to: Jeff H. Duyn, Laboratory of Diagnostic Radiology Research, NIH, Building 10, Room B1N-256, Bethesda, MD 20892.

Received December 15, 1993; revised March 3, 1994; accepted May 15, 1994.

0740-3194/94 $3.00

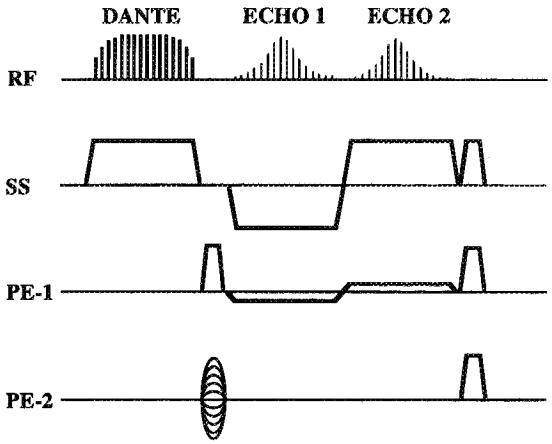


FIG. 1. 3D FS-BURST pulse sequence. The excitation consists of a Hamming-apodized BURST RF-pulse in combination with a slice selection (SS) gradient. Two echo trains (ECHO 1, ECHO 2) are created by repeated gradient reversal. Both echo trains are phase encoded in two directions by PE-1 and PE-2. A gradient crusher is applied after collection of the second echo.

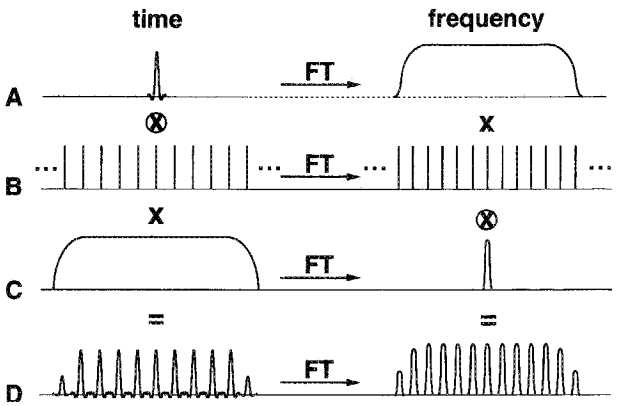


FIG. 2. Principle of BURST excitation. Timing of the BURST RF pulse is given (left), together with corresponding frequency domain signals (right). The BURST pulse was composed of three parts: (a) a shaped RF pulse, (b) a train of evenly spaced delta pulses, and (c) an apodized envelope function. In time domain, these parts were subsequently convolved ($A \otimes B$), and multiplied ($(A \otimes B) \times C$), to yield D. In frequency domain, this corresponds to ($FT(A) \times FT(B)) \otimes FT(C)$, resulting in an array of evenly spaced narrow frequency bands.

overheating of the gradients.

Data processing was performed off-line on Sun-SPARC workstations (Sun Microsystems, Mountainview, CA) using IDL processing software (Research Systems, Boulder, CO). Prior to 3D Fourier transformation, a Hamming filter was applied over 20% of each echo (higher $k$-space points), and over the higher $k$-space points (also 20%) in the second phase encode dimension. This resulted in an effective resolution of $4.5 \times 4.5 \times 4.7$ mm.

## RESULTS

Figure 4 shows a comparison of measurements between conventional BURST and FS-BURST using two different shifting protocols. The measurements were performed on

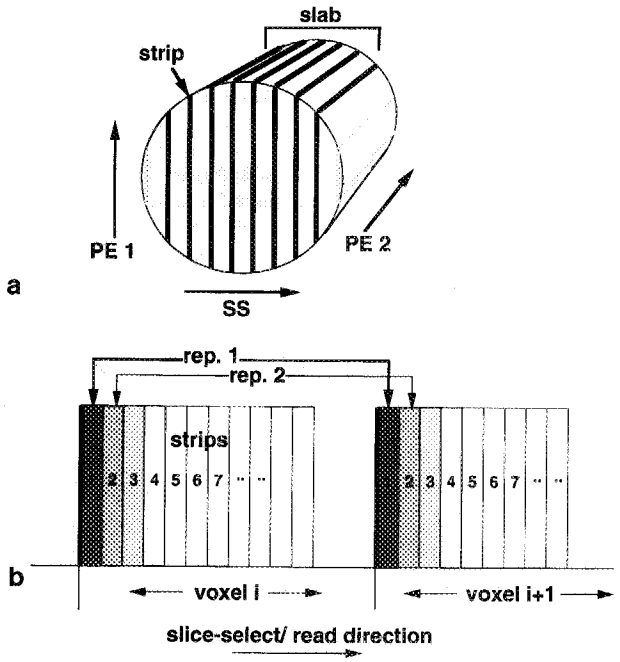


FIG. 3. Strip selection in 3D FS-BURST experiment. (a) Selection of parallel strips within a slab, in a cylindrical object. The strip-shaped regions, excited with the BURST RF pulse, run parallel to phase encoding gradients PE-1 and PE-2, and perpendicular to the slice select (SS) gradient. (b) For each *TR*, a single strip is excited within each imaging voxel. On successive repetitions (e.g., rep. 1 and rep. 2 in the figure), the RF transmitter frequency is shifted, resulting in a shift of the strip locations. The figure illustrates a single strip shift protocol.

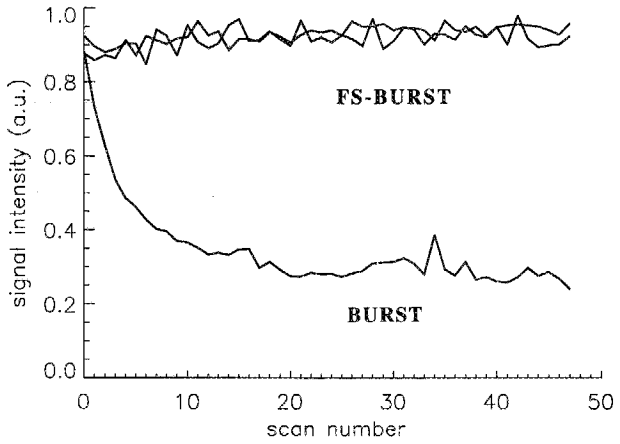


FIG. 4. Comparison of saturation effects in human brain using BURST and FS-BURST. Repeated excitations were performed without phase encoding gradients. A rapid, $T_1$-related decay of magnetization is observed with BURST. A stationary level is reached after approximately 1.3 s. The experiments performed with single- and seven-strip shifted FS BURST (see text) show negligible saturation effects.

a normal volunteer with the phase encoding gradients switched off. The BURST experiment shows a clear decay of the magnetization over time. The amount of signal loss is somewhat smaller than one would estimate based on $T_1$ effects. We attribute this to microscopic motion and diffusion. The loss of magnetization seen in repeated

BURST measurements is not observed with FS-BURST, demonstrating the effectiveness of the shifting principle. Very little difference is seen between single and seven strip shifted FS-BURST, a finding which was also observed in the phase encoded experiments. The effectiveness of the strip shift principle in the phase encoded experiment is demonstrated in images of Figs. 5a and 5b, obtained with the 3D BURST and 3D FS-BURST experiments respectively. FS-BURST shows a clear improvement in image quality and SNR.

Figure 6 shows a comparison between images reconstructed from the second and first echo train, respectively. Although the image reconstructed from the first echo train has a somewhat higher SNR, it shows more distortions related to $B_0$ variations over the object. A phantom measurement without phase encoding gradients shows an equal $T_2$*-weighting for all echoes in the second echo train (Fig. 7). In order to further investigate image quality and SNR, the FS-BURST experiment was repeated 20 times, and the results were averaged (Fig. 8, also Figs. 6c, 6d). Again, no significant difference was observed between the single and seven strip shift protocols. Image SNR was around 55 for gray matter. Note the uniform background noise, indicating minimal image artifacts.

## DISCUSSION

The first 3D data obtained with a BURST-type imaging method are presented. Good quality images of human brain were acquired, demonstrating the validity of the strip-shift principle to reduce saturation effects. Images obtained from the first echo train showed susceptibility related artifacts. This is due to linearly increasing weighting of local $B_0$ variations over the first phase encoding direction. As anticipated, these artifacts were not seen in the images obtained from the second echo train, since equal gradient amplitudes were used during excitation and readout periods.

The reduction of saturation effects with FS-BURST allowed for shortening of $TR$ much beyond $T_1$, thereby increasing efficiency as compared to conventional BURST. The actual gain depends on experimental circumstances such as $TR/T_1$, strip profile, diffusion effects, etc.

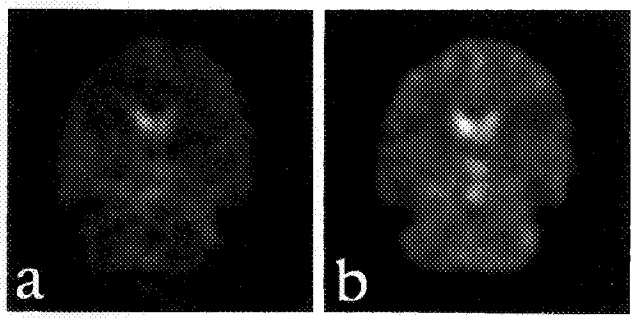


FIG. 5. Comparison of image quality of 3D BURST (a) and 3D FS-BURST (b). Comparison of a single corresponding slice from each dataset demonstrate the increased signal to noise ratio and reduced artifacts of FS-BURST.

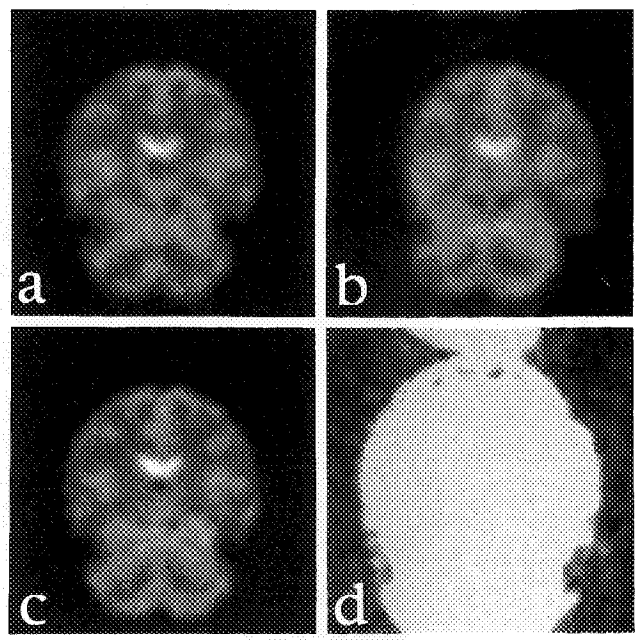


FIG. 6. Image quality of 3D FS-BURST. Single corresponding slices were reconstructed from second (a,c,d) and first (b) echo train. Images (a) and (b) were reconstructed from a single 3D acquisition, whereas in (c) and (d) 20 measurements were averaged. Image (d) shows the noise level of image (c), in order to demonstrate the absence of distinct artifacts.

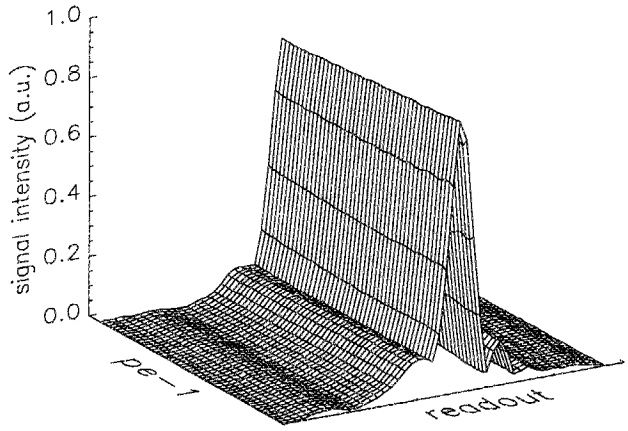


FIG. 7. Signal intensity distribution over the second echo train. The FS-BURST experiment was performed without phase encoding gradients, and without apodization of the BURST RF pulse train. A 3-liter bottle filled with water ($T_1$ = 2.5 s) was used. Although no shimming was performed, a constant signal amplitude over the echo train is observed, indicating identical $T_2$*-weighting for all echoes.

A clear advantage of FS-BURST over other fast imaging techniques is that it is less demanding with regard to gradient slew rates, even at very high imaging speeds. The small number of gradient switchings in BURST imaging lessens demand on gradient slew rates, and reduces eddy current effects. The major physical limitation on further increasing speed is the maximum strength of the read gradient, and the bandwidth of digitizer/receiver combination.

The fact that all echoes of the second echo train have

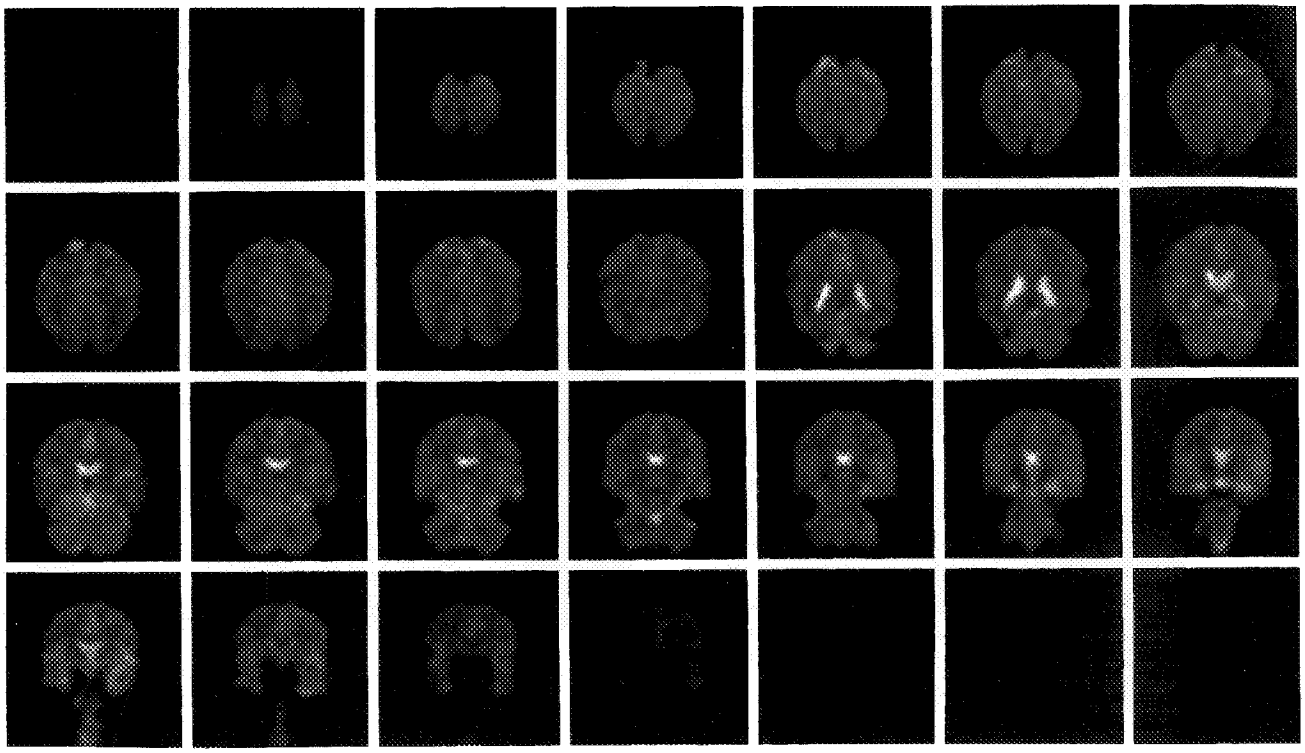

FIG. 8. Consecutive slices through the human brain, obtained with 3D FS-BURST, 20 averages. The images were reconstructed from the second echo train. Note the excellent contrast between gray and white matter.

identical $T_2$*-weighting makes FS-BURST an attractive candidate for susceptibility-based neuro-imaging experiments. Although initial results show good quality susceptibility-weighted images, some further research is required to evaluate stability and reliability of the method. Future developments will partly be geared toward bolus tracking neuro-imaging experiments.

## ACKNOWLEDGMENTS

The authors thank Drs. J. A. Frank and D. Weinberger for their helpful suggestions and support.

## REFERENCES

1. A. Villringer, B. R. Rosen, J. W. Belliveau, J. L. Ackerman, R. B. Lauffer, R. B. Buxton, Y. S. Chao, V. J. Wedeen, T. J. Brady, Dynamic imaging with lantanide chelates in normal brain: contrast due to magnetic susceptibility effects. *Magn. Reson. Med.* **6**, 164–174 (1988).
2. S. Ogawa, T. M. Lee, A. R. Ray, D. W. Tank, Brain magnetic resonance imaging with contrast dependent on blood oxygenation. *Proc. Natl. Acad. Sci. (USA)* **87**, 9868–9872 (1990).
3. P. Mansfield, I. Pykett, Biological and medical imaging by NMR. *J. Magn. Reson.* **29**, 355–373 (1978).
4. A. Haase, J. Frahm, D. Matthei, W. Haenicke, K. D. Merboldt, FLASH imaging. Rapid NMR imaging using low flip-angle pulses. *J. Magn. Reson.* **67**, 258–266 (1986).
5. C. T. W. Moonen, G. Liu, P. van Gelderen, G. Sobering, A fast gradient gradient-recalled MRI technique with increased sensitivity to dynamic susceptibility effects. *Magn. Reson. Med.* **26**, 184–189 (1992).
6. J. Hennig, Fast imaging using BURST excitation pulses, *in* "Proc., SMRM, 7th Annual Meeting, 1988," p. 238.
7. J. Hennig, M. Hoddap, Burst imaging, *MAGMA* **1**, 39–48 (1993).
8. P. Le Roux, J. Pauly, A. Macovski, BURST excitation pulses, *in* "Proc., SMRM, 10th Annual Meeting, 1991," p. 269.
9. I. J. Lowe, R. E. Wysong, DANTE ultrafast imaging sequence (DUFIS). *J. Magn. Reson.* **B 101**, 106–109 (1993).
10. L. Zha, R. E. Wysong, I. J. Lowe, Optimized ultra-fast imaging sequence (OUFIS), *in* "Proc., SMRM, 10th Annual Meeting, 1993," p. 471.
11. G. Bodenhausen, R. Freeman, G. Morris, A simple pulse sequence for selective excitation in Fourier transform NMR. *J. Magn. Reson.* **23**, 171–175 (1976).